2008 IEEE Intelligent Vehicles Symposium
Eindhoven University of Technology
Eindhoven, The Netherlands, June 4-6, 2008

IMMPDA Vehicle Tracking System using Asynchronous Sensor Fusion of Radar and Vision

Feng Liu, Jan Sparbert, and Christoph Stiller

***Abstract*—This paper focuses on recognition and tracking of maneuvering vehicles in dense traffic situations. We present an asynchronous multi obstacle multi sensor tracking method that fuses information from radar and monocular vision. A low level fusion method is integrated into the framework of an IMMPDA Kalman filter. Real world experiments demonstrate that the system combines the complementary strengths of the employed sensors.**

I. Introduction

Advanced driver assistance systems for cars require reliable perception of the vehicle environment. In particular, high-level driving assistance tasks like emergency breaking or full speed range ACC necessitate a level of reliability that may only be achieved through a combination of multiple sensors. Recognizing and classifying of objects on the road as well as determining their position and velocity are the key challenges for numerous applications. Being complementary in nature, radar and monocular vision may yield object detection with high reliability through appropriate information fusion techniques [1]-[2]. The individual properties of radar and vision, as well as their completive potential have been discussed in [3]. Systems using radar and vision fusion differ mainly in their fusion level and in the synchronous or asynchronous processing scheme. Steux and Laurgeau [1] presented in their work a synchronous system with low level fusion. They combined raw data from vision and radar to produce new raw data that are expected to be more informative than the original data. Another synchronous system introduced in [2] uses radar targets to generate the area of interest (AOI) in each image. The detections from these AOI are used to validate the radar targets. In [3] Sole developed a synchronous system with high level fusion, that tracks objects independently by each sensor and subsequently matches, associates and validates the tracks of both sensors.

This contribution proposes asynchronous processing of radar and vision data. In contrast to the previously cited methods, the proposed approach shall meet the following requirements:

1. Object candidates can be initiated from vision data as well as from radar data.
2. The method shall work in the field of view of either sensor, i.e., objects may be updated using either vision data or radar data or both.
3. Objects can be classified and validated using either vision data or radar data or both.
4. Objects can be tracked even in highly dynamic driving maneuvers.

The remainder of the paper is organized as follows: The next section introduces the sensor models for radar and vision as well as the features used for object tracking. In Section 3, an interacting multiple model filter with probabilistic data association IMMPDA is proposed. A multi sensor tracking system using monocular vision and radar is introduced in Section 4. Results from experimental vehicles in natural traffic scenes presented in Section 5 lead to a conclusion and future work.

II. Sensor Models

A. Radar

In our system a 77-GHz long range radar is used. It has a maximum range of 200m and covers an azimuth angle of 10°, cf. [4]. The accuracy of the radar sensor is high in radial direction, i.e. in its measurements of range r and range rate $v = \dot{r}$. In angular direction, the radar provides coarse measurements for the lateral angle α of each object detected. The radial and angular measurements are uncorrelated. Thus, the measurement vector $\mathbf{z}_1$ and the measurement covariance matrix $\mathbf{R}_1$ are given as

$$\mathbf{z}_1 = \begin{pmatrix} r \\ v \\ \alpha \end{pmatrix}, \qquad \mathbf{R}_1 = \begin{pmatrix} \sigma_r^2 & \rho\sigma_r\sigma_v & 0 \\ \rho\sigma_r\sigma_v & \sigma_v^2 & 0 \\ 0 & 0 & \sigma_\alpha^2 \end{pmatrix}, \qquad (1)$$

where $\sigma_r, \sigma_v, \sigma_\alpha, \rho$ denote standard deviations and correlation coefficient of the respective measurements.

B. Camera

We use a monocular camera in our system. The camera has a field of view (FOV) of $\pm 22°$ horizontally and $\pm 16°$ vertically. The image sequence analysis algorithm searches the images for possible objects evaluating a diversity of features, like optical flow, symmetry and shadow. Then these

Feng Liu is with the Driver Assistance Department, Robert Bosch GmbH, 71229 Leonberg, Germany (e-mail: Feng.Liu3@ de.bosch.com).
Jan Sparbert is with the Driver Assistance Department, Robert Bosch GmbH, 71229 Leonberg, Germany (e-mail: Jan.Sparbert@ de.bosch.com).
Christoph Stiller is with the Institute for Measurement and Control Theory, University of Karlsruhe, 76131 Karlsruhe, Germany (e-mail: stiller@mrt.uka.de).

features are fused using the Dempster-Shafer Evidence Theory [5] to detect potential object boundaries. Typically more than one boundary is generated for each vehicle. Each boundary represents a candidate for the lower edge of the object, i.e. the intersection of the object rear with the road plane. This edge is signaled along with its covariance via

$$\mathbf{z}_2 = \begin{pmatrix} p_y \\ p_x \end{pmatrix}, \quad \mathbf{R}_2 = \begin{pmatrix} \sigma_{py}^2 & 0 \\ 0 & \sigma_{px}^2 \end{pmatrix} \tag{2}$$

$$\mathbf{z}_3 = w, \quad \mathbf{R}_3 = \sigma_w^2, \tag{3}$$

where $\mathbf{z}_2$ denotes the pixel coordinates of the objects' lower center, $\mathbf{z}_3$ denotes object width, and $\mathbf{R}_2, \mathbf{R}_3$ denote the respective covariance matrices. The admissible detection range of the image analysis algorithm is restricted to 80m, as the reliability of object detection significantly deteriorates for larger distances.

III. IMM KALMAN FILTER

The interacting multiple model (IMM) Kalman filter has been introduced to cope with abruptly changing dynamical behavior [6]. Recent work on implementation of IMM for real traffic situations has been presented in [7]. The IMM filter used in this paper accounts for typical vehicle maneuvers, such as constant acceleration or constant speed cruising, and the transition between them. It is combined with a probabilistic data association (PDA) scheme as introduced in [8]. The specifics of our IMMPDA filter are presented in the sequel.

A. Dynamic models

As mentioned in the introduction section the key information for advanced driver assistance system is the position and the velocity of the target. An appropriate choice of the coordinate system to represent vehicle dynamics and sensor information is crucial for an appropriate model: While measurement properties of the employed sensors are best represented in polar sensor-fixed coordinates, Cartesian global coordinates are best suited to represent vehicle dynamics. The advantages and disadvantages of Cartesian and polar coordinate system are discussed in [8]. Buehren and Yang [9] present an interesting global coordinate model and provide a comparison between filter results for model representations in sensor-fixed and global coordinate systems. In this paper a representation in semi-global Cartesian coordinates is proposed. After the prediction and innovation steps of the filter have been conducted in global Cartesian coordinates, all information is transformed into a coordinate system moved with the host vehicle.

Two alternative dynamic system models are used in our IMM filter:

1) The first dynamic model assumes constant velocity cruising:

$$\dot{\mathbf{X}}_1 = \tfrac{d}{dt}\begin{pmatrix} x \\ v_x \\ a_x \\ y \\ v_y \\ a_y \end{pmatrix} = \begin{pmatrix} 0 & 1 & 0 & 0 & 0 & 0 \\ 0 & 0 & 0 & 0 & 0 & 0 \\ 0 & 0 & 0 & 0 & 0 & 0 \\ 0 & 0 & 0 & 0 & 1 & 0 \\ 0 & 0 & 0 & 0 & 0 & 0 \\ 0 & 0 & 0 & 0 & 0 & 0 \end{pmatrix}\begin{pmatrix} x \\ v_x \\ a_x \\ y \\ v_y \\ a_y \end{pmatrix} + \begin{pmatrix} 0 \\ \nu_{vx} \\ 0 \\ 0 \\ \nu_{vy} \\ 0 \end{pmatrix}, \tag{4}$$

where ν_{vx} and ν_{vy} denote zero-mean uncorrelated noise of standard deviation σ_{vx} and σ_{vy}, respectively, accounting for the uncertainty in acceleration.

2) The second dynamic model assumes constant acceleration, described by:

$$\dot{\mathbf{X}}_2 = \tfrac{d}{dt}\begin{pmatrix} x \\ v_x \\ a_x \\ y \\ v_y \\ a_y \end{pmatrix} = \begin{pmatrix} 0 & 1 & 0 & 0 & 0 & 0 \\ 0 & 0 & 1 & 0 & 0 & 0 \\ 0 & 0 & 0 & 0 & 0 & 0 \\ 0 & 0 & 0 & 0 & 1 & 0 \\ 0 & 0 & 0 & 0 & 0 & 1 \\ 0 & 0 & 0 & 0 & 0 & 0 \end{pmatrix}\begin{pmatrix} x \\ v_x \\ a_x \\ y \\ v_y \\ a_y \end{pmatrix} + \begin{pmatrix} 0 \\ 0 \\ \nu_{ax} \\ 0 \\ 0 \\ \nu_{ay} \end{pmatrix}, \tag{5}$$

where ν_{ax} and ν_{ay} denote zero-mean uncorrelated noise of standard deviation σ_{ax} and σ_{ay}, respectively, accounting for the uncertainty in jerk.

B. Model interaction

The initial state for prediction of each model is a mixture of the states from the last cycle of all models with the mixing probabilities:

$$\mu_{k-1|k-1}^{i|j} = \frac{1}{c_j} p_{ij} \mu_{k-1}^{i} \quad i, j = 1,2, \tag{6}$$

where μ_{k-1}^{i} is the model probability of the model i in the last cycle and p_{ij} is the probability for the transition from model i to model j. The normalizing constants are

$$c_j = \sum_{i=1}^{2} p_{ij} \mu_{k-1}^{i} \quad j = 1,2. \tag{7}$$

The initial state $X^{0j}_{k-1|k-1}$ and covariance $P^{0j}_{k-1|k-1}$ of the model j are:

$$X^{0j}_{k-1|k-1} = \sum_{i=1}^{2} X^{i}_{k-1|k-1} \mu^{i|j}_{k-1|k-1} \quad j = 1,2 \tag{8}$$

$$P^{0j}_{k-1|k-1} = \sum_{i=1}^{2} \mu^{i|j}_{k-1|k-1} \Big[P^{i}_{k-1|k-1} + \left(X^{i}_{k-1|k-1} - X^{0j}_{k-1|k-1} \right) \cdot \left(X^{i}_{k-1|k-1} - X^{0j}_{k-1|k-1} \right)' \Big] \quad j = 1,2, \tag{9}$$

where $X^{i}_{k-1|k-1}$ and $P^{i}_{k-1|k-1}$ is the state and covariance of the model i of the last cycle.

C. Model filtering

Using the initial state and covariance the predicted states and covariances are calculated in a Kalman filter according to the two motion models. The innovation and state update in the Kalman filter under the different model assumptions will be discussed in Section 4.

D. Model probability update

The calculation of the likelihood function for an IMM filter with PDA has been introduced in [8]. Therefore the likelihood function Λ^{j}_{k} corresponding to the model j is:

$$\Lambda^{j}_{k} = (1 - P_D \cdot P_G) \cdot \beta + \sum_{i=1}^{m} P_D \cdot N(V_{ij}; 0, S_{ij}), \quad (10)$$

where the P_D denotes the detection probability of a target, P_G is the association gate probability, β is the false alarm density, m is the number of the associated measurements of a target and $N(V_{ij};0,S_{ij})$ is a Gaussian distribution for the innovation V_{ij} with zero mean and the covariance S_{ij}.

Thus the updated model probabilities are:

$$\mu^{j}_{k} = \frac{1}{c}\Lambda^{j}_{k}\sum_{i=1}^{2} p_{ij}\mu^{i}_{k-1} \quad j = 1,2, \quad (11)$$

with the normalizing constant

$$c = \sum_{j=1}^{2}\left(\Lambda^{j}_{k}\sum_{i=1}^{2} p_{ij}\mu^{i}_{k-1}\right) \quad (12)$$

E. Estimate and covariance combination

The mixture of the model-conditioned states estimates and covariances yields the resulting system state estimate and covariance according to the mixture equations

$$X_{k|k} = \sum_{j=1}^{2} X^{j}_{k|k}\mu^{j}_{k} \quad (13)$$

$$P_{k|k} = \sum_{j=1}^{2}\mu^{j}_{k}\left[P^{j}_{k|k} + (X^{j}_{k|k} - X_{k|k})\cdot(X^{j}_{k|k} - X_{k|k})'\right]. \quad (14)$$

IV. MULTI SENSOR TRACKING SYSTEM

A. Measurement transformation

We use a linear Kalman filter in Cartesian coordinates. Hence, the measurements from radar and camera are transformed to the Cartesian coordinate model of the system.

The transformation of radar measurements is given by

$$\mathbf{z}_1 = \begin{pmatrix} r \\ v \\ \alpha \end{pmatrix} \Rightarrow \hat{\mathbf{z}}_1 = \begin{pmatrix} x = r\cos\alpha \\ v_x = v/\cos\alpha + v_{x,ego} \\ y = r\sin\alpha \end{pmatrix} \quad (15)$$

$$\hat{\mathbf{R}}_1 = g \cdot \mathbf{R}_1 \cdot g',$$

where $v_{x,ego}$ is the longitudinal velocity of the host vehicle, and the transformation matrix g is defined as

$$g = \begin{pmatrix} \cos\alpha & 0 & -r\sin\alpha \\ 0 & 1/\cos\alpha & v\sin\alpha/\cos^2\alpha \\ \sin\alpha & 0 & r\cos\alpha \end{pmatrix} \quad (16)$$

In [10] Stein presents a method which computes range and range rate using the road geometry and the point of contact of the vehicle and the road in image. According to this method the longitudinal range x and the lateral range y of an object can be computed like below:

$$x = \frac{fH}{p_y \cdot c_p} \quad (17)$$

$$y = \frac{p_x \cdot x \cdot c_p}{f}, \quad (18)$$

where f is the focus length of the camera, H is the height between the camera and ground, p_y and p_x denote the pixel coordinates of the objects' lower center in (2) and c_p is the pixel pitch unit.

The object width can be computed as

$$W = \frac{w \cdot x \cdot c_p}{f} \quad (19)$$

Due to the sensitivity of camera measurements on weather conditions, vertical road curvature and tilt dynamics of the host vehicle, range measurements of the camera may eventually be highly inaccurate. Therefore, in this paper we employ the predicted range value $x_{k|k-1}$ from the initial state $X^{0}_{k-1|k-1}$ of the models in (8) to calculate y and W for each model filter. Thus the transformation of camera position measurements reads

$$\mathbf{z}_2 = \begin{pmatrix} p_y \\ p_x \end{pmatrix} \Rightarrow \hat{\mathbf{z}}_2 = \begin{pmatrix} x = fH/(p_y \cdot c_p) \\ y = p_x \cdot x_{k|k-1} \cdot c_p / f \end{pmatrix} \quad (20)$$

$$\hat{\mathbf{R}}_2 = h \cdot \mathbf{R}_2 \cdot h'$$

with the transformation matrix

$$h = \begin{pmatrix} \frac{fH}{c_p p_y^2} & 0 \\ 0 & \frac{x_{k|k-1} c_p}{f} \end{pmatrix} \quad (21)$$

Likewise, coordinate transformation of the width is given by

$$\mathbf{z}_3 = w \Rightarrow \hat{\mathbf{z}}_3 = W = w \cdot x_{k|k-1} \cdot c_p / f$$
$$\hat{\mathbf{R}}_3 = (\frac{x_{k|k-1} c_p}{f})^2 \cdot \mathbf{R}_3 \quad (22)$$

B. Probabilistic data association

The IMM algorithm requires that the used motion models have identical validation regions in measurement space. In this paper, we use the combined state prediction of the system given by

$$X_{k|k-1} = \sum_{j=1}^{2} X^j_{k|k-1} c_j \quad (23)$$

$$P_{k|k-1} = \sum_{j=1}^{2} c_j \left[P^j_{k|k-1} + (X^j_{k|k-1} - X_{k|k-1}) \cdot (X^j_{k|k-1} - X_{k|k-1})' \right], \quad (24)$$

where $X^j_{k|k-1}$ and $P^j_{k|k-1}$ denotes the predicted state and covariance of the model j whereas c_j is the predicted model probability from Eq. (7).

Radar measurements are associated to targets using a validation gate as described in [11] with a gate probability set to 0.98.

The association of camera measurements to targets is a little more complex. The targets are at first transformed to boundaries in each image following Eqs. (17), (18) and (19). Target boundaries are associated with camera measurements if they match with the respective measurement boundary. Two special cases are explicitly considered:

1) If a target is occluded by another target closer to the host vehicle in image, we impose that only the closer one is seen by the camera.
2) In praxis a radar reflection may come from any possible matters on the road, like vehicles, trees or cola cans. In order to prevent that a moving vehicle may be assumed to be occluded by nearby stationary objects, we impose that moving targets may not be occluded by stationary targets.

The PDA procedure yields the association probabilities of the measurement with the targets as outlined [11].

C. Asynchronous filtering

The notion of synchrony in the context of multi sensor tracking systems my refer to sensors or to the tracking process itself:

1) Synchrony of sensors
   In a synchronous sensor system all sensors take every measurement at the same time instant. In contrast asynchronous sensors operate independently and often even at different measure rates.
2) Synchrony of tracking
   A synchronous tracking system predicts or retrodicts measurements or objects that may be taken at different time instances into pseudo measurements or objects that are aligned in time [12]. In contrast, asynchronous tracking systems employ every measurement or object upon availability to validate and initiate its tracks.

A main drawback of synchronous tracking system against asynchronous system is the loss of sensor information when several measurements are "compressed" into a pseudo measurement. Furthermore, prediction or retrodiction of sensor information introduces additional noise to the overall system. Last not least, the additional time delay of a synchronous system may be prohibitive for the functionality of safety relevant advanced driver assistance systems.

For the sake of modularity, sensors typically operate independent of another and hence provide asynchronous data. The radar and camera used in our system measure objects independently. The radar has a measurement rate of 10 Hz while the camera operates at 25 Hz. To achieve maximum flexibility of the tracking system we have developed an asynchronous tracking system with low level data fusion for the asynchronous sensors. This allow for full exploitation of sensor information and mixing of sensor information at an early stage of the analysis procedure. Because the processing time the radar sensor is significantly larger than the processing time of the camera sensor (Fig. 1), the tracking system receives the radar measurements after the camera measurements even when the radar and camera sensors begin their measurements simultaneously. This problem is well discussed in [13]. A theoretically optimal solution as well as a cost-effective approximation thereof is presented in [14]. To resolve the problem we store all received measurements of the camera into a buffer that is read out when new measurements of the radar arrive. Then the tracking system can process the buffered camera data and the just received radar data sequentially in the order of their measurement times. This process is shown in Fig. 2.

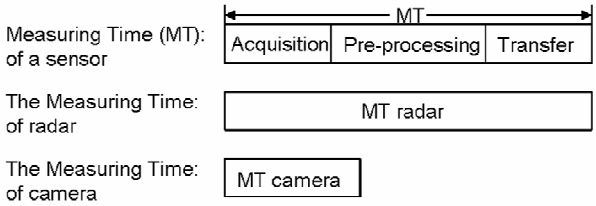

Fig. 1. The measuring time of radar and camera

D. Target recognizing and validation

When a target is measured by the camera we use the width information to classify the target as a passenger car, truck or a motorcycle. Furthermore we calculate a probability of track existence for each target using the integrated PDA (IPDA) introduced in [15].

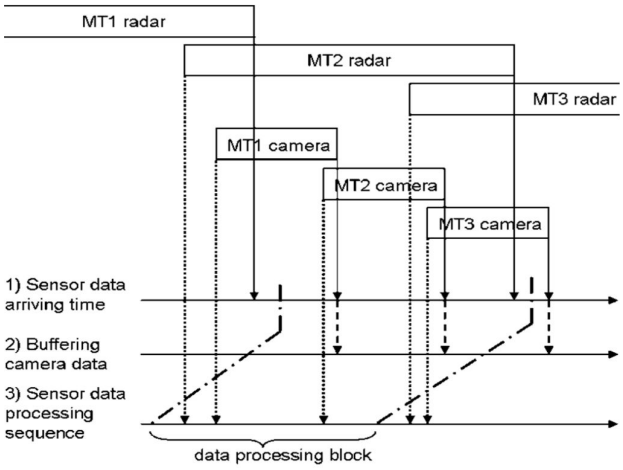

Fig. 2. Asynchronous sensor data processing

1) Radar data and camera data arrive at the tracking system
2) All camera data MT1, MT2 and MT3 camera are buffered.
3) The radar data MT2 radar and the camera data MT1 and MT2 camera, which arrived in the system between the arriving times of MT1 radar and MT2 radar, build a data processing block that is processed sequentially in the order of measurement by the tracking system.

V. RESULTS

The evaluation of the multi sensor system is based on data recorded from driving on highways and in urban areas. The radar measurements and camera images were recorded together with the longitudinal speed of the host vehicle.

The constant velocity model of IMM is parameterized as:

σ_{vx} =1m/s^2 and σ_{vy} =1m/s^2

The constant acceleration model is parameterized as:

σ_{ax} =100m/s^3 and σ_{ay} =50m/s^3

The transition matrix of the IMM filter is set to

$$pM(0.1s) = \begin{pmatrix} 0.98 & 0.02 \\ 0.02 & 0.98 \end{pmatrix}.$$

The initiation values of the models are 0.2 for the CV model and 0.8 for the CA model.

Fig. 3. The target is measured by both, the radar and the camera. The boundaries depict the measurements provided by the camera sensor and the triangle depicts the radar detection. The cross show the target tracked by the proposed method.

Fig. 4. The target is turning left and is only measured by the camera.

Figs. 3 and 4 show results from a typical urban driving scene where a vehicle is followed by the host vehicle. Figs. 5 - 8 show the tracked parameters together with the measurements. Using the information of the camera sensor the target is also correctly classified as passenger car with a width of 1.55 meter.

VI. CONCLUSIONS

In this paper we present an IMMPDA multi sensor tracking system using asynchronous processing of measurements of radar and vision. The result of the simulation using measurements in real traffic situations shows that the tracking system combines the advantages of both sensors and the IMM works correctly. In Fig. 8 we can see that the range measurements of camera are unreliable over a distance of 35 meter due to pitch dynamics of the host vehicle. Even though the proposed system copes well with this situation, future work on image stabilization could contribution to directly improve the measurement data. In particular, this will enhance the tracking performance for targets that are only measured by the camera.

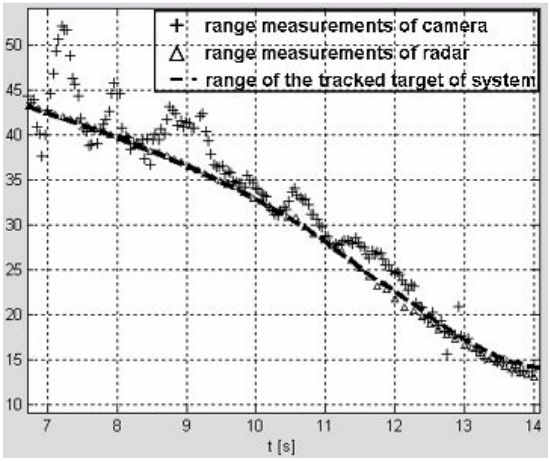

Fig. 5. Tracked range of the target in [m].
Due to its high accuracy the tracked range is dominated by the range measurements of the radar.

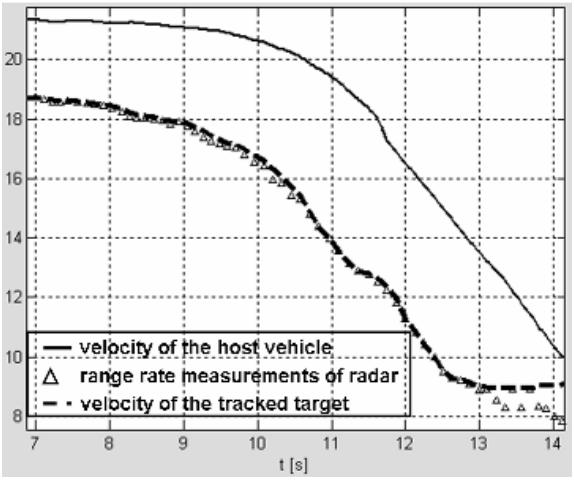

Fig. 6. Tracked velocity of the target in [m/s]. Only the radar can measure the velocity instantaneously. At the 10.5 s and 12 s the target brakes strongly. Between 11.2 s and 11.5 s and from 13 s onwards the target cruises at almost constant velocity.

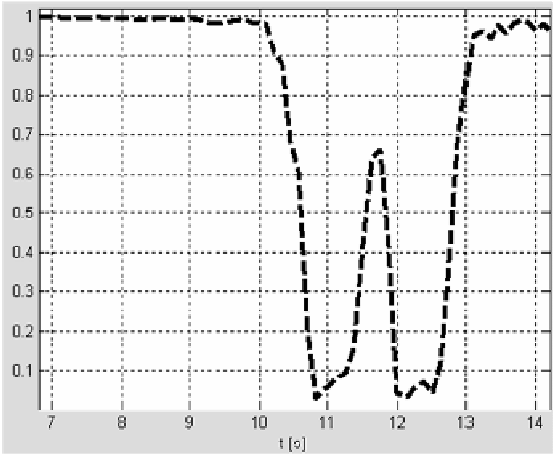

Fig. 7. Model probability of the constant velocity model. At the 11 s and 12 s the IMM filter switches from constant velocity model to constant acceleration model.

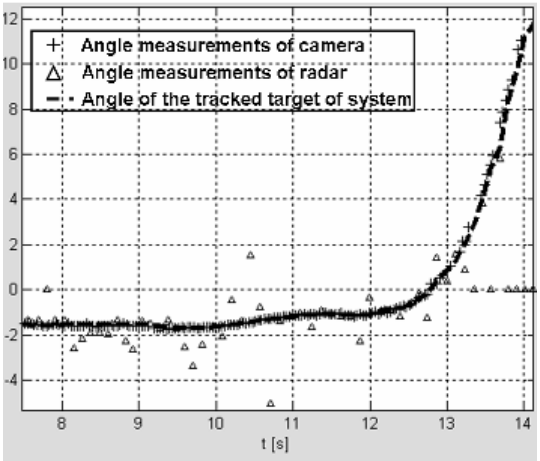

Fig. 8. Angle in [°] computed from the tracked lateral distance range. Due to its high accuracy the tracked angle is dominated by the camera measurements.

REFERENCES

[1] B. Steux, C. Laurgeau, L. Salesse, and D. Wautier, "Fade: A vehicle detection and tracking system featuring monocular color vision and radar data fusion," *in Proc. IEEE Intell. Vehicles Symp., Versailles, France, Jun. 2002*, pp. 632-639

[2] G. Alessandretti, A. Broggi, and P. Cerri, "Vehicle and Guard Rail Detection Using Radar and Vision Data Fusion," IEEE Trans. Intell. Transp. Systems, Vol. 8, No. 1, March 2007.

[3] A. Sole, O. Mano, G. P. Stein, H. Kumon, Y. Tamatsu and A. Shashua, "Solid or not solid: Vision for radar target validation," in Proc. IEEE Intell. Vehicles Symp., Parma, Italy, Jun. 2004, pp. 819-824.

[4] Robert Bosch GmbH and H. Bauer, Adaptive Fahrgeschwindigkeitsregelung ACC, Chrisiani, Konstanz, 2002.

[5] S. Simon, W. Niehsen, A. Klotz and B. Lucas, "Video-basierte Objekt-Detektion und Verifikation von Radar-Objekt-Hypothesen für Komfort- und Sicherheitsfunktionen," in Workshop Fahrerassistenzsysteme FAS 2005, Germany, Apr. 2005.

[6] H. A. P. Blom, An efficient filter for abruptly changing systems. In Proc. IEEE Conf. on Decision and Control, pp. 656-658, 1984.

[7] N. Kaempchen, K. Weiss, M. Schaefer and K. C. J. Dietmayer, "IMM object tracking for high dynamic driving maneuvers," in IEEE Intell. Vehicles Symp., Parma, Italy, Jun. 2004, pp. 825-830.

[8] S. Blackman and R. Popoli, Design and Analysis of Modern Tracking Systems, artech house ed., Norwood, MA, 2000.

[9] M. Buehren and B. Yang, "A Global Motion Model For Target Tracking in Automotive Applications," in Proc. IEEE intl. Conf. On Acoustics, Speech and Signal, Hawaii, Apr. 2007, Vol. 2, pp. 313-316.

[10] G. P. Stein, O. Mano, and A. Shashua, "Vision-based ACC with a single camera: bounds on range and range rate accuracy," in Proc. IEEE Intell. Vehicles Symp., Columbus, Ohio, Jun. 2003, pp. 120-125.

[11] Y. B. Shalom and T. E. Fortmann, Tracking and Data Association, Academic Press INC., Orlando, 1988.

[12] X. Lin, Y. B. Shalom and T. Kirubarajan, "Multisensor-Multitarget Bias Estimation for General Asynchronous Sensors," IEEE Trans. On Aerospace and electronic systems, Vol. 41, No. 3, Jul. 2005.

[13] N. Kaempchen and K. C. J. Dietmayer, "Data synchronization strategies for multi-sensor fusion," in Proc. of ITS 2003, 10th World Congress on Intelligent Transportation Systems, Madrid, Spain, Nov. 2003.

[14] Y. Bar-Shalom, H. Chen, and M. Mallick, "One-step solution to the multi-step out-of-sequence measurement problem in tracking," IEEE Trans. Aerospace and Electronic Systems, vol. 40, pp. 27-37, 2004.

[15] D. Musicki, R. Evans and S. Stankovic, "Integrated Probabilistic Data Association," IEEE Trans. On Automatic Control, Vol. 39, No. 6, Jun. 1994.